Original Research Paper

The enantioselective enhancing effect and mechanistic insights of chiral enhancers in transdermal drug delivery

Yang Zhang[a,1], *Chao Liu*[a,1], *Dongxiao E.*[b], *Wenxuan Jia*[a], *Peng Sun*[a], *Hui Li*[a], *Guojing Yu*[a], *Peng Quan*[a], *Mingzhe Liu*[b,*], *Liang Fang*[a,*]

[a] *Department of Pharmaceutical Sciences, Shenyang Pharmaceutical University, Shenyang 110016, China*
[b] *Department of Organic Chemistry, Shenyang Pharmaceutical University, Shenyang 110016, China*

ARTICLE INFO

ABSTRACT

Overlook of chiral consideration in transdermal drug delivery increases administrated dose and risk of side effects, decreasing therapeutical effects. To improve the transdermal delivery efficiency of eutomer, this work focused on investigating the law and mechanism of enantioselective enhancing effects of chiral permeation enhancers on drug enantiomers. Chiral nonsteroidal anti-inflammatory drugs and terpene permeation enhancers were selected as model drug and enhancers. The results indicated that the L-isomer of permeation enhancers increased the skin absorption of S-enantiomer of drug and D-isomer improve the permeation of R-enantiomer, in which the enhancement effect (ER) of L-menthol on S-enantiomer (ER = 3.23) was higher than that on R-enantiomer (ER = 1.49). According to the pharmacokinetics results, L-menthol tended to enhance the permeation of S-enantiomer better than R-enantiomer (2.56 fold), and showed excellent *in vitro/in vivo* correlations. The mechanism study showed that L-isomer of permeation enhancers improved the permeation of S-enantiomer by increasing the retention, but the D-isomer by improving partition for better permeation. Enantioselective mechanism indicated that the weaker chiral H-bond interaction between drug-chiral enhancers was caused by the enantiomeric conformation. Additionally, stronger chiral enhancers-skin interaction between L-isomer and S-conformation of ceramide produced better enhancing effects. In conclusion, enantioselective interaction of chiral drug-chiral enhancers and chiral enhancers-chiral skin played a critical role in transdermal drug delivery, rational utilization of which contributed to improving the uptake of eutomer and inhibiting distomers to decrease a half of dose and side effects, increasing transdermal therapeutical efficiency.

* Corresponding authors.
E-mail addresses: mz_liu03@163.com (M. Liu), fangliang2003@yahoo.com (L. Fang).
[1] These authors contributed equally to this work.
Peer review under responsibility of Shenyang Pharmaceutical University.

1. Introduction

Chemical permeation enhancers (CPEs) play an indispensable role in the transdermal drug delivery system (TDDS) in favor of weakening the skin barrier to increase permeation of drug. The terpene CPEs is widely utilized in the TDDS ascribing to its high potency and low toxicity [1]. However, the terpene CPEs contained at least one chiral center which result in different permeation enhancing effects because of multiple enantiomers [2]. On the other hand, according to the statistics, more than half of drugs used for transdermal delivery are chiral [3], in other words, that in the form of racemate are actually impure when the biological activity of the drug is relevant to one of the enantiomers—eutomer, threatening to increase the side effects and decrease therapeutical effects [4,5]. Especially, the enantioselective therapeutical differences would expand for TDDS formulated with the stereoisomeric compositions, including chiral drug and chiral chemical permeation enhancers (CCPEs). These chiral components in the formulation greatly influence therapeutical effects of the transdermal preparation that inhibit the uptake of eutomer and increase that of distomers [6–8]. The S-timolol was used for the treatment of essential hypertension, however, D-limonene enhanced the skin permeation of R-timolol (5-fold) to a greater extent than S-timolol (2-fold) [9], which meant the higher uptake of distomers (R-isomer) increased the risk of side effects and decreased the therapeutical efficiency [10–12]. The transdermal delivery of nonsteroidal anti-inflammatory drugs (NSAIDs) allows patients to obtain longer-lasting pain relief compared with the other administrated routes [13]. Actually, the anti-inflammatory activity of NSAIDs was ascribed to the S-enantiomer, while the R-enantiomer hardly showed the effect. Additionally, intake of R-ibuprofen would result in kidney perfusion, water sodium retention [14,15]. Thus, the proper choice of CCPEs contributes to the more highly efficient transdermal delivery of S-enantiomer and decreasing a half of administrated dose to avoid the unnecessary side effects and irritation. Unscientific combination of chiral drug and CCPEs increases the uncertainty of transdermal delivery of eutomers and limits the development of TDDS.

The key consideration of influencing the delivery efficiency of TDDS with chirality includes: (i) press-sensitive adhesive (PSA), (ii) physicochemical properties of drugs, (iii) types of CPEs, (iv) the barrier function of skin. Usually, a pair of enantiomers share the identical physicochemical properties in the achiral environment, however, they would perform the different properties, such as solubilities, partition behaviors, enantioselective release from the medium, under the conditions of chiral environments, in which the phenomenon was more apparent in TDDS. Commercially available acrylate PSA widely applied in TDDS, without chiral functional groups, struggled to influence the chiral drug. Moreover, the CPEs in transdermal formulation not only change the release of drugs, but also increase the retention amount in skin. Especially, terpene CPEs with chiral centers and chiral drugs coexisted in a transdermal preparation, which provide the chiral environment to influence the enantioselective release and skin permeation. In fact, the chirality of skin also give

rise to the enantioselective differences for the chiral drug. We previously verified that S-flurbiprofen was easier to permeate into the skin than R-flurbiprofen because stronger interaction with the chiral ceramide in stratum corneum (SC) [16]. Overlooking these chiral factors have serious impacts on the therapeutical effects in TDDS, increasing administrated dose and risk of side effects. Therefore, chirality in drug, CPEs and skin has to be considered in order to develop the highly efficient chiral TDDS. As a result, investigation of the law of enantioselective permeation enhancing effects of CCPEs on drug enantiomers and clarification of molecular mechanism was not only in favor of screening proper CCPEs for desired eutomers and avoid the side effects that distomoer brought, but also provide the theorical basis and design space for the development of more highly efficient CCPEs and chiral drugs utilized in TDDS.

In this work, we investigated the law of enantioselective permeation enhancing effects of CCPEs on chiral drugs and clarified the molecular mechanism by selecting chiral α-arylpropionic acids NSAIDs—ibuprofen (IB), flurbiprofen (FP) and naproxen (NP) enantiomers as model drugs, and D- or L-menthol (MEN), limonene (LIM) and linalool (LIN) enantiomers as model CCPEs. Enantioselective effects of CCPEs on drug enantiomers were found in vitro and in vivo and showed in vitro/in vivo correlations (IVIVC). The enantioselective enhancing effect of CCPEs enantiomers on drug enantiomers were characterized from viewpoints of chiral interaction of drug-CCPEs and chiral interaction of CCPEs-skin. The mechanism relevant to the chiral interaction strength and chiral binding site of FP and MEN enantiomers was investigated by circular dichroism (CD), ^{13}C NMR, molecular docking (MD). Mechanism of CCPEs-skin interaction was characterized by Attenuated Total Reflection Fourier transform infrared spectroscopy (ATR-FTIR), Small-angle X-ray scattering (SAXS), differential scanning calorimetry (DSC), atomic force microscope (AFM) and molecular dynamic simulation studies. The work was to propose the novel insight into transdermal delivery strategy of chiral drug with CCPEs and clarified the mechanism of enantioselective effects of CCPEs on drug enantiomers. It was expected to improve the efficiency of transdermal delivery of S-enantiomer with anti-inflammatory activity to decrease the side effects originated from R-enantiomer including dizziness and urinary tract infection. This study laid a theoretical basis and design space for development the transdermal patches with chiral drugs and chiral excipients.

2. Materials and methods

2.1. Materials

R-ibuprofen (R-IB), S-ibuprofen (S-IB), R-flurbiprofen (R-FP), S-flurbiprofen (S-FP), R-naproxen (R-NP) and S-naproxen (S-NP) were purchased from Hengyuan Technology Co., Ltd. (Hubei, China); Caprylic/capric triglyceride (ODO) was obtained from Yousuo Chemical Factory Co., Ltd. (Shandong, China); D-menthol (D-MEN), L-menthol (L-MEN), D-limonene (D-LIM), L-limonene (L-LIM), D-linalool (D-LIN), L-linalool (L-LIN) were all obtained from Macklin Biochemical Co., Ltd.

(Shanghai, China). DuroTak® 87–4098 and DuroTak® 87–2852 were purchased from Henkel Corp (New Jersey, USA); The release liners (Scotchpak™ 9744) and backing film (Scotchpak™ 9680) were obtained from 3 M Co., Ltd. (St. Paul, USA); All other chemicals and solvents were analytical reagent grade.

2.2. Preparation of rat skin

Male Wistar rats (180–220 g) were purchased from the Experimental Animal Center of Shenyang Pharmaceutical University (Shenyang, China). All procedures observed the NIH Guidelines for the Care and Use of Laboratory Animals, and were approved by the Animal Ethics Committee of Shenyang Pharmaceutical University (approval SYPU-IACUC–C20226–1–18). The abdominal hair of rat skin was removed by clipper (model 900, TGC, Japan) and an electrical shaver (Braun 190, Germany) after the rat was anaesthetized by the urethane solution (1.5 ml, 20%, w/v). Then the rat was sacrificed by cervical dislocation to excise the abdominal site using the surgical scissor to obtain the skin sample followed by subcutaneous fat tissue removed with the tweezer and scalpel [16].

2.3. In vitro skin permeation and release study of patch with chiral drug and CPEs

The transdermal patch with drug enantiomers mixed CCPEs was prepared to investigate the enantioselective enhancing effects of CCPEs. Firstly, 0.015 g R- or S-enantiomer of drug (3%, w/w) and 0.015 g of CCPEs (3%, w/w) were dissolved in ethyl acetate (200 µl) and then the mixture was added in commercially available pressure sensitive adhesive (PSA) (DuroTak® 87–4098) (0.5 g) with constantly stirring (2 h) under room temperature conditions. Subsequently, the PSA with FP enantiomers was coated onto a release liner by a film applicator with 0.45 µm. The coated release liner was then dried at 50 ºC for 10 min before being laminated with a backing film. The resulting patch was cropped into a circular piece with dimensions of 12 mm, while maintaining a thickness within the range of 80–90 µm. The Franz diffusion cell was utilized to perform the *in vitro* skin permeation and release study. And 4 ml PBS (pH 7.4) was selected as the receptor vehicle and stirred constantly during the study. Each group was replicated for three times ($n = 3$). The receptor vehicle (2 ml) was withdrawn at predetermined time (2, 4, 6, 8, 10, 12 h) and then 2 ml fresh PBS was added in the receptor side in time. Finally, the sample was injected into HPLC to analyze after filtered by millipore filter (0.22 µm).

In vitro release study was conducted to observe the impact of different CPEs enantiomers on release of drug enantiomers. The donor and receptor vehicle were the same as above, except replacing the skin with semipermeable membrane (Cellophane® membrane of MWCO 500). Each group was replicated for three times ($n = 3$). The receptor vehicle (2 ml) was withdrawn at the 0.5, 1, 1.5, 2, 3, 4, 6, 8, 10, 12 h and fresh PBS (2 ml) was added in the receptor side. Finally, the sample was filtered by millipore filter (0.22 µm) before they were analyzed by HPLC. The cumulative transdermal permeation amount was calculated by concentration and volume of each sample point [17]:

$$Q = \frac{\sum_{i=2}^{n} 2.5C_i - 0.5C_{i-2}}{A} (i = 2, 4, 6 \cdots) \quad (1)$$

where Q_{patch} was the cumulative transdermal permeation amount (µg/cm^2), C_i was concentration of drug in receptor solution (µg/ml) at time i (h) and A was effective permeation area (1.13 cm^2).

The enhancement ratio of drug skin permeation (ER) was calculated as follows:

$$ER = \frac{Q_{with\ enhancer}}{Q_{without\ enhancer}} \quad (2)$$

2.4. Retention amounts of FP and CCPEs in different skin layers

Retention of FP and CPEs in skin were investigated following the transdermal permeation experiments [17]. In brief, the skin was taken down from the Franz diffusion cell and cleaned by cotton wool with 10% of methanol. Then the skin was weighted followed sealed in the EP tube, where 1 ml methanol was added in advance. Finally, the sample was treated with ultrasound for 1 h to extract the FP and CCPEs retaining in skin. The mixture was centrifuged at 16,000 rpm for 5 min to obtain the supernatant. And then supernatant was analyzed by the HPLC and GC method in Supplymentary information. Each group was replicated for three times ($n = 3$).

Retention of FP and MEN in SC and epidermis (EP) (herein including viable epidermis and dermis) was also determined. The skin was stripped for 7 times after transdermal permeation for 8 h to obtain SC sample. And then the skin sample was sealed in the tube containing 4 ml methanol and subjected to ultrasound for 1 h. The rest part of skin defined as the EP was performed in line with above. Each group was replicated for three times ($n = 3$). Samples were centrifuged at 16,000 rpm for 5 min and the supernatant was analyzed by HPLC and GC method in Supplymentary information.

2.5. Partition study of drug enantiomers and CCPEs

The ratio of drugs and enhancers distribution study was performed after the skin retention study. Drugs and CCPEs were collected in skin and processed as the same as method 2.4. Additionally, the residue drug and CCPEs in patch were also collected and analyzed by HPLC and GC method. The distribution ratio was calculated by dividing drug and enhancer concentrations of each part by initial drug and enhancer, respectively. Each group was replicated for three times ($n = 3$).

2.6. Determination of activation energy of transdermal permeation

In vitro transdermal permeation experiments were identical with method 2.3, but they were performed at 28, 32, 36, 40 and 44 °C, respectively. Permeability coefficients were calculated according to permeation plots to obtain activation energies at various temperatures by Arrhenius relationship [15]. The

activation energy of transdermal permeation was calculated by the Arrhenius equation as follows:

$$\text{Log } K_p = \frac{E_{act}}{2.303RT + \log K_{p0}} \tag{3}$$

Where E_{act} was the activation energy, R is gas constant (1.987 kcal/mol), and T was the temperature, K_{p0} was the Arrhenius constant.

2.7. In vitro release and skin permeation of transdermal patch formulated with FP enantiomers and l-men

Transdermal patches were prepared with R- or S-FP and L-MEN to verify the L-MEN enantioselective permeation enhancing effects in practice use for following establishment of the IVIVC in pharmacokinetic study. The PSA (DuroTak® 87–2852) was selected as the matrix originating from the carboxyl group of it which satisfied the higher drug loading for the better therapeutical effects. And then the drug loading was 10% (w/w) and the that of L-MEN was 10% (w/w). The preparation method and procedure were the same as 2.2. Each group was replicated for six times ($n = 6$). In vitro transdermal permeation and release experiments were carried out as method 2.3. Each group was replicated for six times ($n = 6$).

2.8. Pharmacokinetic study

The pharmacokinetic study of transdermal patch was conducted to investigate the enantioselective permeation enhancing effects of L-MEN on FP enantiomers in vivo. Rats were allowed free access to food and water throughout the study. They were divided into two groups, in which one group was given patches formulated with FP enantiomers (20 cm^2, 15 mg, $n = 6$) and anther group was administrated with patches formulated with FP enantiomers and L-MEN (20 cm^2, 15 mg, $n = 6$). Orbital blood was sampled at 0.5, 1, 2, 4, 8, 12, 24, 30, 36 and 48 h. For i.v. administration, FP enantiomers were dissolved in 0.1 mol/l NaOH solution to prepare the drug solution with concentration of 10 mg/l and pH was adjusted to 7–8. Rats were given either R-FP (10 mg/kg, $n = 6$) or S-FP (10 mg/kg, $n = 6$) by tail vein injection. The orbital blood was sampled (0.4 ml) at 0.2, 0.3, 0.5, 0.75, 1, 2, 3, 4, 6, 8, 10, 12 and 24 h. Then plasma sample was obtained after the blood sample was centrifuged at 16,000 rpm at 25 °C for 3 min. Subsequently, 20 μl internal standard solution (Diclofenac, 0.5 μg/ml), 1 ml acetonitrile and 20 μl HCl (0.1 mol/l), 100 μl plasma sample were mixed. The mixture was vortex mixed for 5 min and centrifuged at 16,000 rpm at 4 °C for 5 min. The supernatant was collected and dried under a stream of nitrogen gas at 50 °C. Subsequently, the dried sample was dissolved by 100 μl mobile phase and filtrated by 0.22 μm millipore filter. Then it was analyzed by HPLC method.

A two-compartment open model was utilized to analyze the data of in vivo transdermal permeation. The plasma concentrations with time were fitted to a biexponential equation derived from the two-compartment open model:

$$C = A \cdot e^{-\alpha t} + B \cdot e^{-\beta t} \tag{4}$$

where C represented the plasma concentration, t represented the time, α, β, A and B represented the hybrid parameters referring to the characterization of distribution and elimination phase.

IVIVC were performed by Phoenix® 64 software. Firstly, the deconvolution was carried to calculate cumulative transdermal absorption from in vivo data. The corresponding unit impulse response (UIR) was obtained from vein injection data to deconvolved. And then the cumulative transdermal absorption in vivo at each time interval was express as fraction of the transdermal delivery dose. Additionally, the fractions of in vitro transdermal permeation were also plotted. Finally, the correlation was established between in vitro transdermal permeation versus the transdermal permeation in vivo.

2.9. Characterization of chiral drug-CCPEs interaction

2.9.1. ^{13}C NMR experiments
Drugs and CCPEs were dissolved in NMR tubes, of which deuterated chloroform acted as solvents. ^{13}C NMR spectra were recorded by Advance 600 MHz spectrometer (Bruker) with tetramethylsilane as internal standard.

2.9.2. Molecular docking (MD)
MD (Materials studio software, version 7.0) was performed to further investigate the mechanism of selectively enhancing permeation of drug enantiomers. The Forcite moule was used to optimize the spatial geometry of structures of CCPEs and drug enantiomers. The Blend Module was utilized to dock and investigate the H-bond interaction between CCPEs and drug enantiomers at COMPASS II force filed.

2.9.3. Measuring the CD spectra of interaction between FP enantiomers and chiral men
CD spectra were used to investigate the changes of chirality after the interaction between FP and MEN enantiomers. The sample was dissolved in methanol to form the drug solution (1 mg/ml) with or without the consistent concentration of MEN enantiomers. And then the CD spectra were recorded on a MOS-500 Spectrometer from 200−380 nm. The spectra were accumulated four times with a bandwidth of 2.0 nm.

2.10. Characterization of CCPEs-skin interaction

2.10.1. ATR-FTIR spectroscopy
ATR-FTIR spectroscopy was utilized to clarify permeation enhancing effects of D- and L-MEN on lipids. The full-thickness rat skin was taken down from the Franz diffusion cell after in vitro transdermal permeation. Then the skin was placed on the ZnSe crystal. The ATR-FTIR spectra was recorded with an average of 60 scans and resolution of 4 cm^{-1}, in the wavenumber range of 4000–500 cm^{-1} by IR spectrometer (NEXUS + 70, Thermo Electron Corporation, Waltham, MA, USA) [17].

2.10.2. SAXS study
The SAXS was carried out to clarify the chiral interaction between CCPEs and lipids in SC. The full-thickness rat skin

was immersed in physiological saline (pH .4) with trypsin (10%, w/v) at 37 °C for 12 h. Then tweezers were utilized to pick up the SC from the skin. Subsequently, purified water was used to rinse the SC sample and dried in vacuum [17]. The obtained SC was treated with drug solution (1 ml), which contained 3% of R- or S-FP and 3% of CCPEs and ethanol as solvents, in order to ensure the same thermal activity with that *in vitro* transdermal permeation. And then the processed SC was experimented by SAXS (Anton Paar, Graz, Austria) with 40 kV/50 mA at 25 °C after the SC sample was dried. The exposure time was 15 min.

In this experiment, the lamellar repeat distance after the FP enantiomers and chiral MEN was calculated by the Bragg's Law:

$$S = (2/\lambda) \cdot \sin\theta \tag{5}$$

$$2d\sin\theta = n\lambda \tag{6}$$

Where d is the lamellar repeat distance) of silver behenate, and 2θ is the scattering angle, S was lattice spacing and the n represented the order of diffraction.

2.10.3. DSC study of SC
The SC sample was processed with the same as method 2.10.2 to obtain dried SC sample which has been treatment with the drug and CCPEs. Approximately 3–5 mg SC sheet was placed in Mettler® alumina crucible (40 µl/6 mm×1.7 mm). The SC sample was heated from 25 to 100 ºC at rate of 10 ºC/min and DSC curves were recorded by Mettler-Toledo thermal analyzer (DSC1, Metter-Toledo International Inc., Zurich, Switzerland) [18].

2.10.4. AFM experiments
AFM was utilized to observe the change of surface morphology of SC after addition of FP and MEN enantiomers [19]. The skin sample was processed as the same as method 2.10.1. The surface morphology of SC was obtained by 5500 AFM/STM system (Agilent, Palo Alto, CA) with tapping mode (2.4 V, 167.88 kHz).

2.10.5. Molecular dynamics simulation (MDS)
MDS (Materials Studio software, version 7.0) was carried to characterize the interaction strength by calculating cohesive energy density (CED) among drug enantiomers, CCPEs and lipids in SC. The Forcite module was used to optimize the structure by COMPASS II force field. Amorphous Cell module

was utilized to construct the lipids model of SC. The system was equilibrated in NVT (50 ps) and NPT (50 ps) at 305 K and 101.325 kPa with a time step of 1 fs. CED was calculated by Materials studio 7.0.

2.11. Statistical data analysis

All statistical calculations were performed by SPSS 17.0. One-way analysis of variance (ANOVA) was used to analyze experiment data. A probability of $P < 0.05$ was taken as significant difference.

3. Results and discussion

3.1. In vitro transdermal permeation of drug enantiomers of patch following by addition of CCPEs

Cumulative permeation profiles of drug enantiomers with different CCPEs were illustrated in Fig. 1. The CCPEs had enhancing effects on drug enantiomers, but to different degree. It was observed that both of L-isomer of CCPEs enhanced the S-enantiomer of drug but the L-MEN had the best significant effects on S-conformation and the D-isomer enhanced the R-enantiomer, in which D-MEN enhanced the permeation remarkably. L-MEN would be more favor of enhancing the skin permeation of S-enantiomer than that of R-enantiomer ($\Delta Q_{IB} = 25.42 \pm 4.52$, $\Delta Q_{FP} = 35.34 \pm 3.52$, $\Delta Q_{NP} = 38.55 \pm 8.52$ µg/cm^2) ($P < 0.05$). On the other hand, D-MEN performed the stronger enhancing effects on R-enantiomers than that of S-enantiomer ($\Delta Q_{IB} = 21.62 \pm 5.44$, $\Delta Q_{FP} = 16.51 \pm 4.12$, $\Delta Q_{NP} = 18.49 \pm 6.85$ µg/cm^2) ($P < 0.05$). The permeation ratio (ER) about the enantioselective permeation enhancing effects on drug enantiomers was listed in Table 1, which showed the higher ER values of L-MEN on S-enantiomers and that of D-MEN on R-enantiomers.

3.2. In vitro release study from the patch

The *in vitro* release study was performed in order to investigate whether enantioselective permeation enhancing effects were caused by the release of drug enantiomers from the patch (Fig. 2). It was observed that the addition of CCPEs increased the release of drug enantiomers. The transdermal or release process depended on the passive diffusion which meant the higher concentration gradient, faster and more

Table 1 – Transdermal permeation data of drug enantiomers with L-MEN and D-MEN.

|	Drug	Cumulative permeation (µg/cm^2)		Flux (µg/cm^2/h)		K_p x 10^3 (cm/h)		ER	
		R	S	R	S	R	S	R	S
L-MEN	IB	44.96±7.32	70.38±8.94	3.41±0.23	6.23±0.39	1.33±0.10	2.44±0.21	2.87±0.08	3.40±0.12
	FP	25.53±6.65	57.87±5.62	2.53±0.33	5.05±0.30	0.98±0.16	1.97±0.13	1.92±0.22	3.17±0.15
	NP	55.98±7.32	94.53±8.96	6.78±0.31	3.23±0.34	2.65±0.30	1.27±0.35	1.74±0.28	2.24±0.33
D-MEN	IB	60.34±3.11	38.73±5.65	5.31±0.32	3.33±0.29	2.09±0.20	1.31±0.11	2.51±0.06	1.99±0.21
	FP	35.61±3.88	20.87±2.87	2.96±0.43	1.74±0.28	1.16±0.11	0.57±0.12	3.23±0.11	1.49±0.16
	NP	82.77±7.99	69.63±6.96	6.90±0.23	5.79±0.44	2.72±0.36	2.28±0.39	2.79±0.31	1.66±0.36
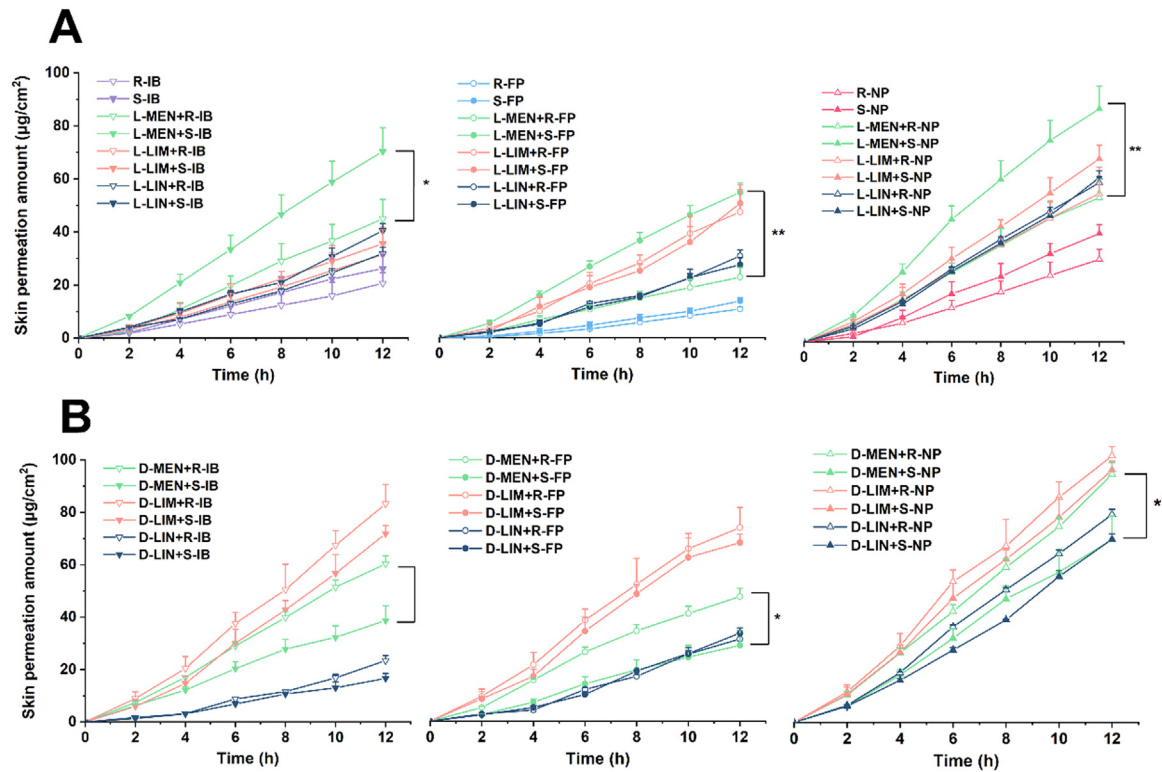
Fig. 1 – *In vitro* permeation profiles of drug enantiomers with (A) L-isomer and (B) D-isomer of CCPEs (*n* = 3), *P < 0.05, **P < 0.01.
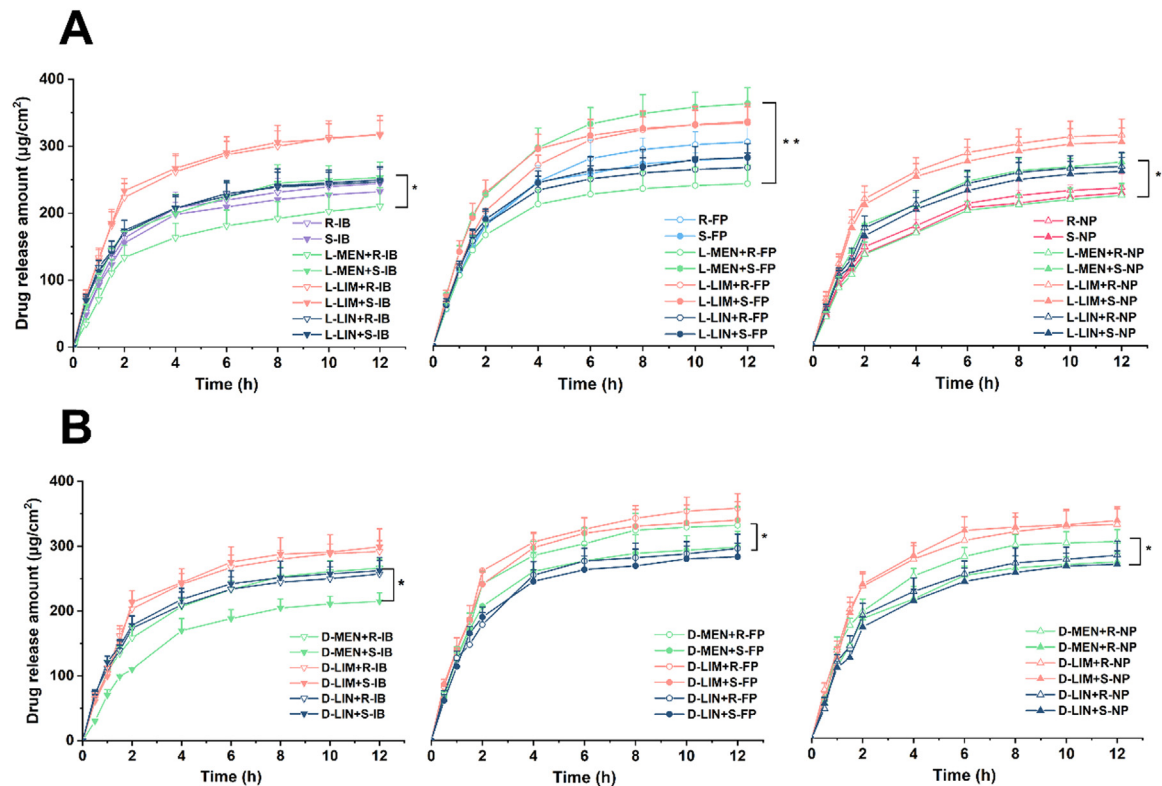

Fig. 2 – *In vitro* release profiles of drug enantiomers with (A) L-isomer and (B) D-isomer of CCPEs (*n* = 3), *P < 0.05, **P < 0.01.
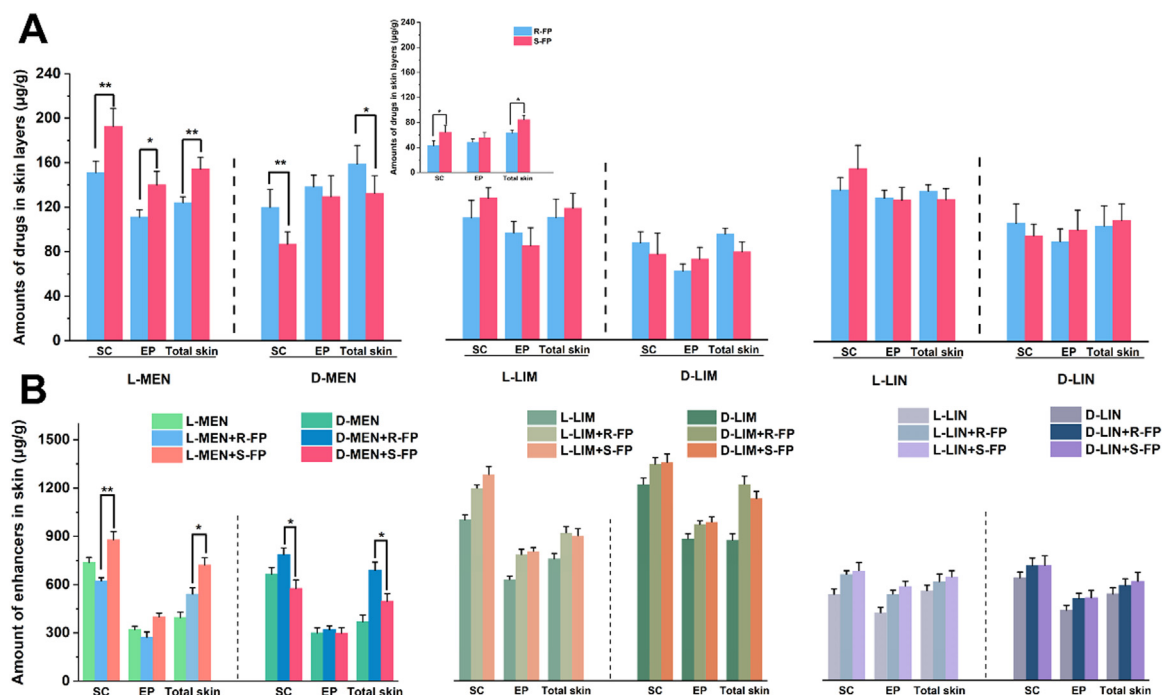
Fig. 3 – Retention amount of (A) FP enantiomers and (B) CCPEs in skin ($n = 3$) *$P < 0.05$, **$P < 0.01$.

permeation or release amount. And thus, release amount drug enantiomers were improved after addition of CCPEs. However, the release amounts of enantiomers showed significant differences following by mixing with the D- or L-isomer. Additionally, the presence of optical isomers of MEN showed different inhibition effects on a pair of drug enantiomers. It was observed that in the case of L-MEN, S-enantiomers were easier to release from the drug-CPEs system enantiomers ($\Delta R_{IB} = 19.60 \pm 4.66$, $\Delta R_{FP} = 116.67 \pm 23.52$, $\Delta R_{NP} = 49.64 \pm 7.76$ μg/cm^2) ($P < 0.05$), contrast to the results of presence of D-MEN that R-enantiomers was more relaxed ($\Delta R_{IB} = 34.88 \pm 6.43$, $\Delta R_{FP} = 38.58 \pm 11.23$, $\Delta R_{NP} = 39.64 \pm 6.63$ μg/cm^2), which suggested that the different interaction existed between drug enantiomers and MEN enantiomers. Other CCPEs did not give rise to the different release from the PSA.

3.3. Retention amount of FP enantiomers and CCPEs

According to the results of transdermal permeation and release, L-isomer of CCPEs showed similar enantioselective enhancing effects on S-enantiomer of drug and D-isomer of CCPEs performed better effects on R-enantiomer (Figs. 1 and 2, Table 1). In addition, IB, FP and NP had the same chiral structure—chiral α-arylpropionic acids. On the other hand, FP was a commonly used NSAID in clinical practice because of its excellent anti-inflammatory effects. Therefore, the FP enantiomers was chosen to further clarify the enantioselective permeation enhancing effects of CCPEs. The retention amount of FP and CPEs enantiomers in skin was carried out to study the different influence of them on skin (Fig. 3). The addition of CCPEs was capable of increasing the

retention in the skin, but MEN and LIN enantiomers showed stronger ability than LIM enantiomers (Fig. 3A). In other words, the chiral MEN and LIN focused on increasing retention of drug in skin to improve permeation, not for the LIM. More importantly, L-MEN was more favor of increasing the retention of S-FP, but D-MEN tended to increase that of R-FP. In terms of identical drug enantiomer, L-MEN had stronger effects of increasing retention than D-MEN. The permeation enhancing effects of terpene CPEs relied on their retention amount in skin [20]. On the other hand, the retention of LIM into the skin was far higher than other CCPEs (Fig. 3B). According to the results, it concluded that LIM enantiomers were much easier to release from the transdermal patch, which indicated that they were able to decrease the retention of drug enantiomers, facilitating transdermal permeation. However, chiral LIM also failed to give rise to the enantioselective interaction with chiral FP because of the absence of different retention amount.

3.4. Partition study of FP enantiomers and CCPEs

In order to more clearly observe the distribution behavior of drug enantiomers in the presence of different CCPEs, the distribution study of FP enantiomers was performed and the results were shown in Fig. 4. It was observaptaraed that L-isomer of CCPEs was able to facilitate the retention in the skin and D-isomer of CCPEs would further increase the permeation by improvement of partition. In detail, L-isomer was easier to retain in skin to increase the amount of S-enantiomer drug in SC, in which L-MEN significantly enhanced the S-enantiomers. On the other hand, however, D-isomer was in more favor of facilitating the R-enantiomer to transfer from SC into receptor medium for better permeation
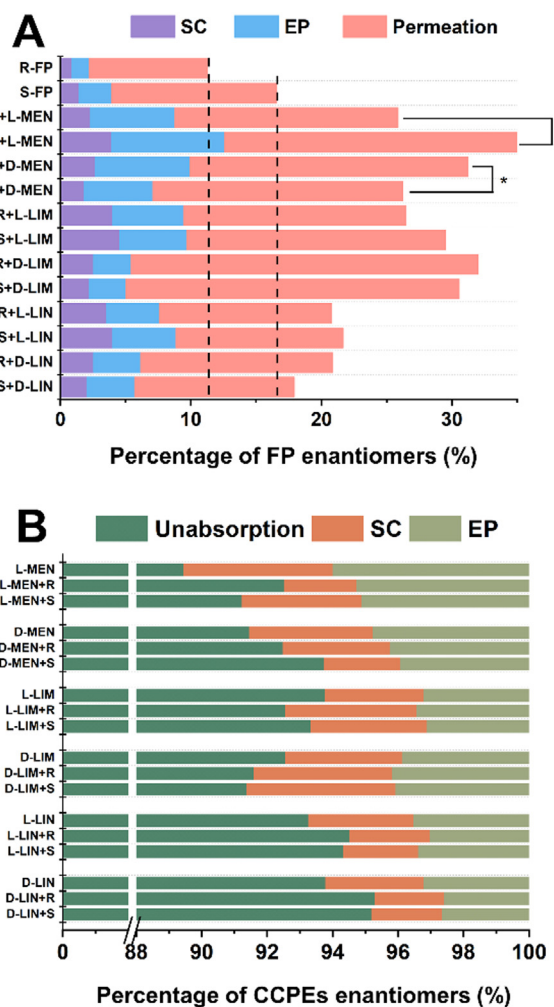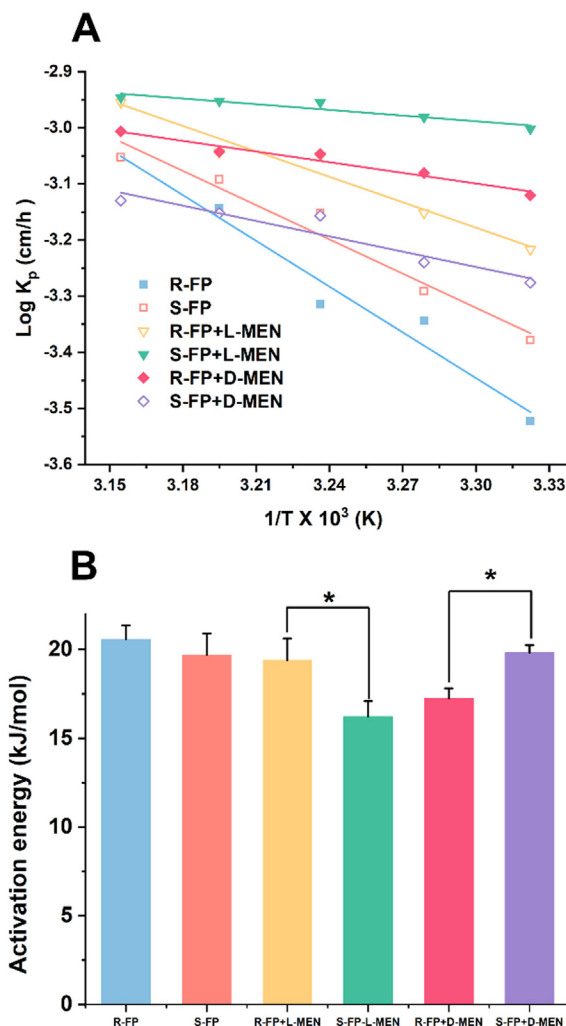
Fig. 4 – (A) The percentage of the FP enantiomers in skin and permeation, (B) The percentage of CCPEs in the unabsorbed, skin retention and skin permeation.

Fig. 5 – Transdermal Arrhenius plots of FP enantiomers with or without L- and D-MEN ($n = 3$).

accompanied with lower retention, where D-MEN was more obvious (Fig. 4A). In the case of MEN enantiomers, the partition of FP enantiomers was improved. On the contrary, partition of MEN enantiomers was inhibited and it performed the enantioselectivity that L-MEN was easier to enhance the skin permeation of S-FP and D-MEN was favor of enhancing permeation of R-FP. And thus, the different interaction occurred between chiral MEN and FP enantiomers to give rise to different impacts on FP enantiomers and MEN enantiomers, respectively. For chiral LIM, the addition of it in transdermal formulation facilitated the partition of drug and itself significantly toward skin. On the contrary, the chiral LIN inhibited the partition of itself (Fig. 4B). It was noted that the amount of vaporized menthol was less than 1% compared with the originally prepared patch in this study, thus we divided the vaporized part into the unabsorption.

### 3.5. Arrhenius plots and calculation of activation energy

The transdermal activation energies of FP enantiomers after addition of L- and D-MEN were calculated for further analysis of chiral interaction. The activation energies of transdermal permeation were thought as the energies that demanded to make drug molecules free of hydrogen bonds from matrix and permeate through the lipid bilayer [21]. The activation energies of FP enantiomers permeation were calculated by Eq. (3) and results were shown in Fig. 5. The transdermal activation energy of R-FP and S-FP was 20.58 ± 0.78 and 19.70 ± 1.22 kJ/mol, respectively. When MEN enantiomers were added, the activation energies significantly decreased. To be specific, for L-MEN, the activation energies of R-FP and S-FP permeation were 19.40 ± 1.23 and 16.22 ± 0.87 kJ/mol, respectively. But those of R-FP and S-FP permeation decreased to 17.25 ± 0.56 and 19.82 ± 0.43 kJ/mol in the presence of D-MEN. The results indicated that permeation activation energies of S-FP were lower in the presence of L-MEN, but that of R-P were lower in the case of D-MEN. The permeation enhancers could weaken the barrier of SC to reduce the activation energy of drug permeation and increase the permeation amount. It concluded that the more L- or D-MEN retained in the SC, resulting in the increased permeation and enantioselective enhancing effects.
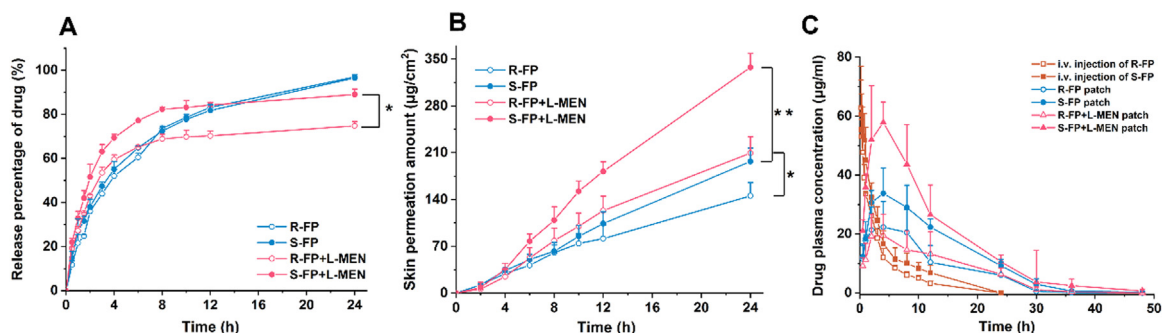
Fig. 6 – The optimized formulation patch of FP enantiomers (A) *in vitro* **release profiles, (B)** *in vitro* **skin permeation profiles, and (C)** *in vivo* **permeation profiles (n = 6).**

Table 2 – Pharmaceutical parameters for FP enantiomers with L-MEN following transdermal administration (mean±SD, n = 6).

Parameter	R-FP	S-FP	R-FP+L-MEN	S-FP+L-MEN
AUC (mg/l·h)	341.89±156.14	570.35±6.25	331.11±141.41	849.93±141.77
MRT (h)	9.84±1.60	11.21±0.33	11.14±0.63	11.52±1.94
$T_{1/2}$ (h)	4.01±0.61	4.84±0.20	4.40±0.73	6.03±1.70
T_{max} (h)	4.67±3.06	4.78±3.11	3.00±1.16	3.33±1.16
CL (l/h/kg)	0.17±0.07	0.09±0.02	0.18±0.09	0.06±0.01
C_{max} (mg/l)	22.47±8.58	38.09±4.52	20.56±7.87	68.83±14.06

3.6. In vitro and in vivo skin permeation of patch with FP and l-men enantiomers

We further investigated the impact of chiral environments provided by the MEN enantiomers on FP enantiomers *in vivo* for better application and verification in aspects of formulation. On one hand, FP was commonly used NSAIDs in clinic and S-FP has been commercially available. On the other hand, L-MEN was acknowledged as a topical analgesic in pharmacy by USA Food and Drug Administration [22]. Therefore, FP enantiomers and L-MEN were chosen as the model drugs and CPEs, and the results were shown in Fig. 6. It was found that L-MEN did influence the release of FP enantiomers from the patch (Fig. 6A). However, compared with the release of drug enantiomers from the results of above, addition of L-MEN decreased the release of FP enantiomers. In fact, different from the above matrix, the CPEs would compete the interaction sites of PSA containing carboxyl groups with drugs, restraining the release of drugs [23]. Additionally, it was easier for L-MEN to enhance the skin permeation of S-FP (ER = 1.78 ± 0.32) than that of R-FP (ER = 1.44 ± 0.22) (Fig. 6B). Even though *in vivo*, S-FP was also enantio–selectively enhanced by the L-MEN (Fig. 5C) and the relevant parameters were listed Table 2. Interestingly, L-MEN rarely enhanced the skin permeation of R-FP *in vivo*. The high IVIVC (R^2 =0.9856, 0.9531, 0.9788 and 0.9783, respectively) indicated that L-MEN could selectively facilitate the skin permeation of S-FP (Table 3).

3.7. Characterization of chiral drug-CCPEs interaction

3.7.1. ^{13}C NMR experiments

^{13}C NMR spectroscopy was performed to investigate the chiral interaction. The results and structures of FP and CPEs

Table 3 – IVIVC between *in vitro* **percent of drug permeation (X) and** *in vivo* **percent of drug absorption (Y).**

Transdermal formulation	IVIVC model	R^2
R-FP	$Y = 2.725+1.788X–0.042 \times ^2$	0.9856
S-FP	$Y = 9.392+1.673X–0.039 \times ^2$	0.9531
R-FP+L-MEN	$Y = 8.196+0.967X–0.012 \times ^2$	0.9788
S-FP+L-MEN	$Y = 11.165+2.041X–0.033 \times ^2$	0.9783

were shown in Fig. 7 and S1. The peaks at 179.98 and 179.97 ppm corresponded to the carboxyl carbon of R-FP and S-FP. Additionally, peaks at 71.55 and 73.53 ppm corresponded to the carbon attached to the hydroxy group of L-MEN and L-LIN. It was found that FP enantiomers were able to form the H-bond interaction with CCPEs except the L-LIM which did not contain hydrogen bond donor (HBD) or hydrogen bond acceptor (HBA) (Fig. 7A). Carbon of carboxyl moved to the lower chemical shift, but carbon connected with the hydroxy of MEN tended to move in opposite directions. In the process of H-bond formation, electron cloud density around the H-bond acceptor decrease and shielded effects were weakened, increasing chemical shift. Accordingly, the results showed that H-bond interaction take place between carboxyl group of FP and hydroxy group of L-MEN or L-LIN, where hydroxy section of carboxyl group acted as HBD and the oxygen atom of CCPEs acted as HBA.

The chemical shift changes of mixture of R-FP and L-MEN (178.41, 71.75 ppm) was more obvious than that of S-FP and L-MEN mixture (179.02, 71.67 ppm) (Fig. 7A). On the contrary, in the case of D-MEN, S-FP (179.02, 71.72 ppm) tended to interacted with it than R-FP (179.29, 71.69 ppm) (Fig. S1). Interestingly, it was found that the chemical shift in the
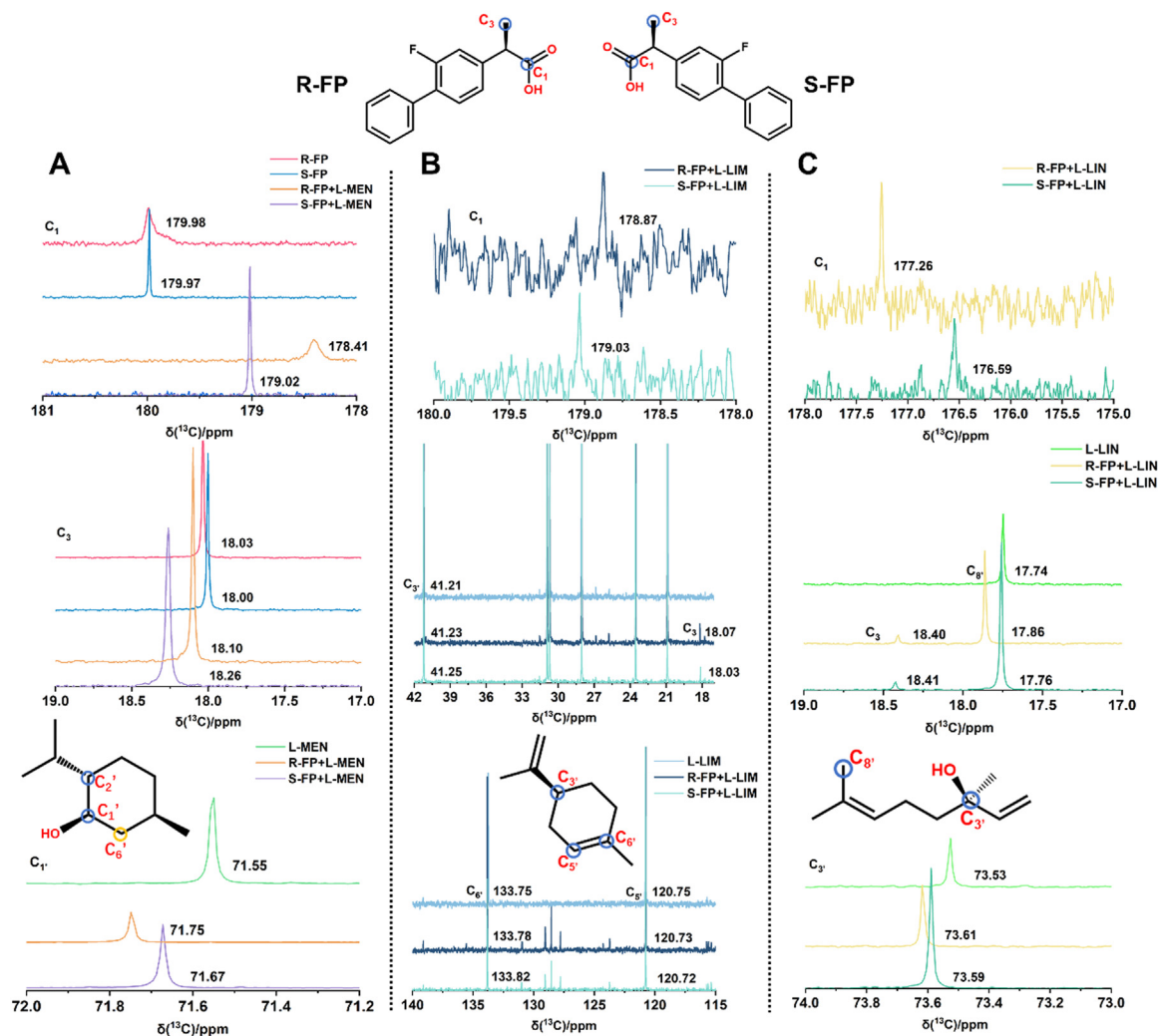
Fig. 7 – ^{13}C NMR spectra of FP enantiomers with (A) L-MEN, (B) L-LIM, (C) LIN.

methyl carbon attached to the chiral carbon of FP changed significantly under the condition of L-MEN, but not for D-MEN. To be specific, chemical shift of methyl group in R-FP changed from 18.03 to 18.10 ppm and that in S-FP moved from 18.00 to 18.26 ppm after mixing with L-MEN. Thus, the position of methyl group connected with chiral carbon in FP was a key to reveal the different interaction between drug enantiomers and L-MEN. However, the chemical shift barely changed following the addition of D-MEN. In other words, methyl group was not the key factor for them, but in relation to both of chiral structure of D-MEN and FP enantiomers. In the case of the L-LIN, the significant differences failed to be observed after interaction with the FP enantiomers even if the H-bond formed between. The single chiral centers struggled to cause the different interaction because a pair of drug enantiomers was capable of forming the most stable H-bond with the L-LIN by selecting the best spatial location for the optimized conformation.

3.7.2. MD
MD was applied to visualize and detail the different interaction caused by steric configuration. Fig. 8 showed the

different H-bond interaction strength reflected by the distance of H-bond between the HBD and HBA. The results were consistent with the ^{13}C NMR result that FP acted as the HBD and CPEs as the HBA. Oxygen atom of L-MEN showed the closer distance with the R-FLU (3.736 Å) than that with the S-FLU (3.274 Å), which revealed the stronger H-bond interaction occurred between the L-MEN and R-FP in Fig. 8A. On another hand, D-MEN performed the stronger interaction with S-FLU (3.401 Å) than that with the R-FLU (3.839 Å) (Fig. S2).

It deserved a note that the methyl group attached to the C_2 of S-FP located closer to the L-MEN when the formation of H-bond, while that of R-FP did not, in the case of L-MEN. On the other hand, isopropyl group of $C_{2'}$ of D-MEN hindered the H-bond interaction strength for the R- and S-FP because of its large molecular volume. And thus, the spatial location for the carboxyl group of FP decided the H-bond strength between FP and D-MEN which was more conductive to the S-FLU to interact. Interestingly, FP enantiomers failed to form H-bond interaction with the L-LIM without HBA or HBD, and thus, it was unable to perform the enantioselectively permeation effects (Fig. 8B). Additionally,
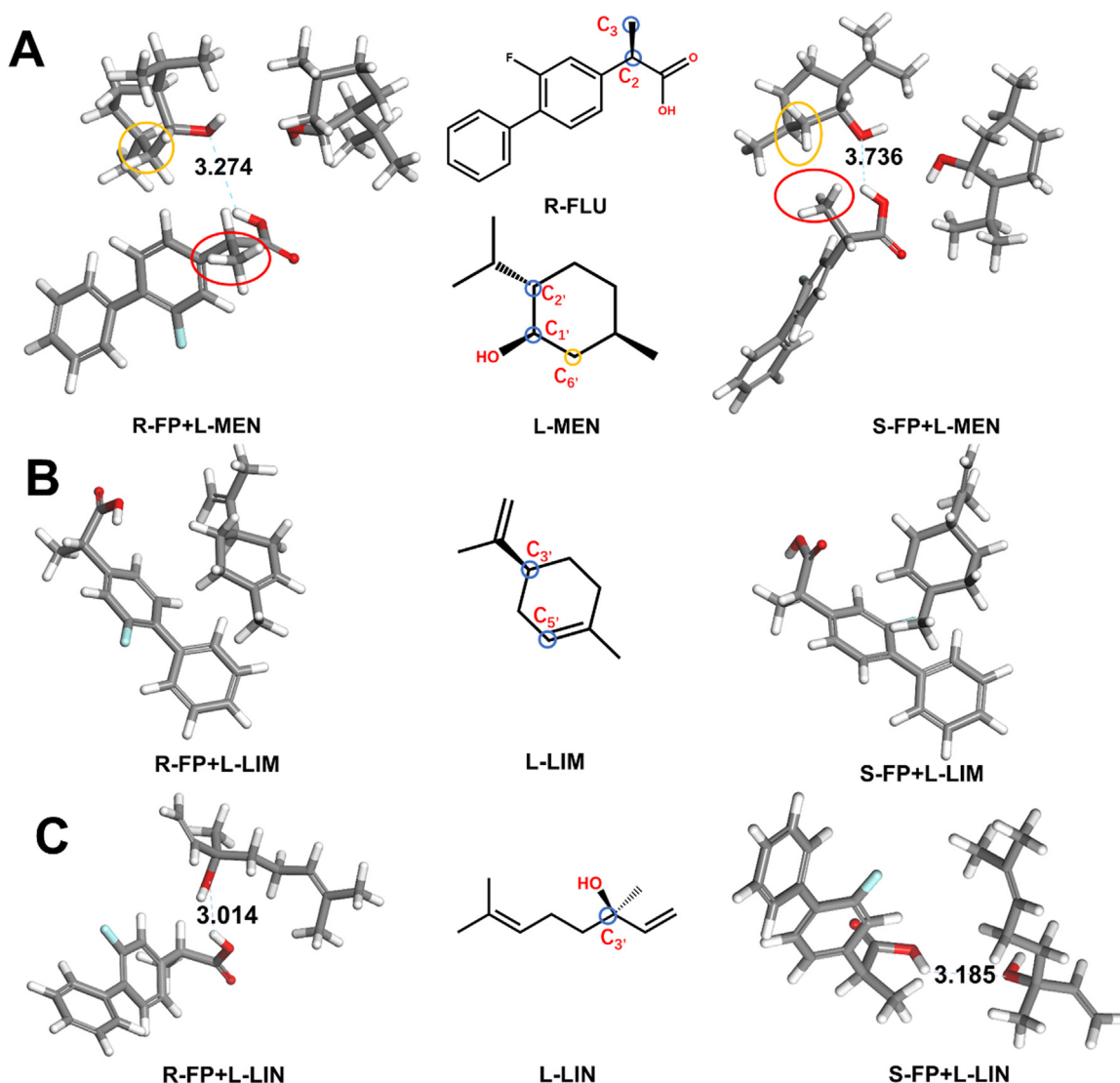
Fig. 8 – Minimum energy complexes of FP enantiomers with (A) L-MEN, (B) LIM, and (V) L-LIN.

despite the formation of H-bond occurring between FP enantiomers and L-LIN (Fig. 8C), the interaction strength was similar, in other words, enantioselective interaction struggled to occur in L-MEN with one chiral center.
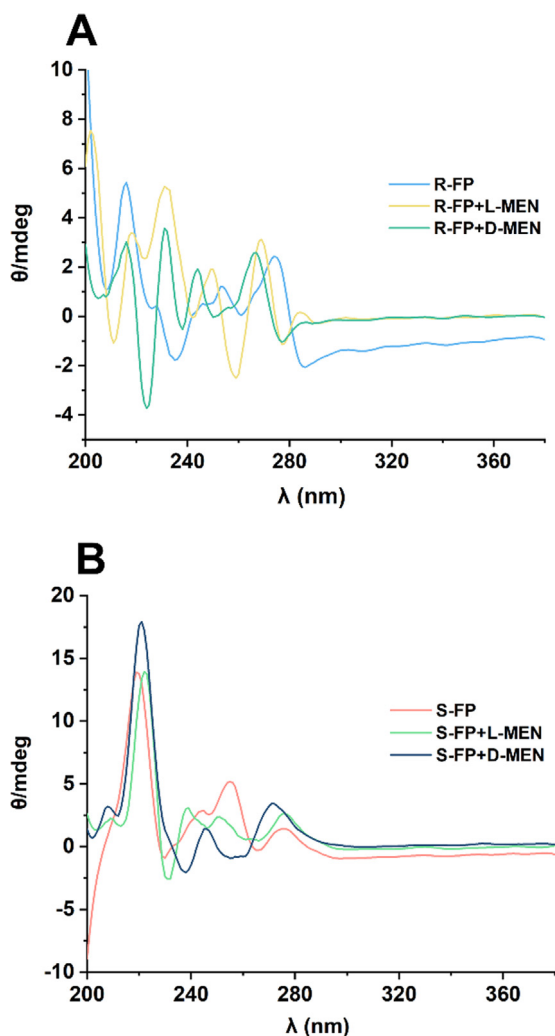
3.7.3. CD spectra

The intrinsic CD of R-FP and S-FP dissolved in methanol located in 200−240 nm and 280 nm regions, respectively. The negative signal of R-FP and positive signal of S-FP was at 208 and 219 nm (Fig. 9). The CD signal of both n, π^* and π, π^* band becomes more intense because of chiral interaction between FP and MEN enantiomers conformational constrains. On one hand, the band of R-FP in 208 nm increased significantly following interacting with the L-MEN, not only that, the increase of peak intensity indicated the higher asymmetry compared with the S-FP. On the other hand, the stronger interaction between S-FP and D-MEN increased its peak intensity in 219 nm and significant shift in 280 nm. The results of CD spectra showed that the interaction between chiral FP

and MEN was influenced by the chiral spatial conformation, but also it disturbed the electron cloud density surrounding the interaction groups.

3.8. Characterization of CCPEs-chiral skin interaction

3.8.1. ATR-FTIR spectroscopy

The ATR-FTIR was used to shed light on the mechanism of selective enhancement of MEN enantiomers from the viewpoint of the skin. The CH_2 asymmetric stretching vibration ($v_{as}CH_2$) was originated from the endogenous lipids in SC and the peak of it was at 2920 cm^{-1}. And thus, the motion of $v_{as}CH_2$ reflected the magnitude of impact of ceramides disturbed by menthol [24]. The results were shown in Fig. 10A. There was no obvious change at 2920.49 cm^{-1} after addition of R-FP and S-FP. However, the movement of $v_{as}CH_2$ after addition of S-FP and L-MEN ($\Delta v_{as}CH_2 = 2.99$ cm^{-1}) was higher than that of $v_{as}CH_2$ after addition of R-FP and L-MEN ($\Delta v_{as}CH_2 = 1.42$ cm^{-1}). The results implied that the addition of

Fig. 9 – CD spectra of chiral MEN with FP enantiomers (A) R-FP (B) S-FP.

S-FP and L-MEN had a greater impact on lipids than that of R-FP and L-MEN. Additionally, D-isomer of CCPEs also disturb the lipids, combination of D-MEN and R-FP better than that with S-FP (Fig. S3). By comparison, L-isomer of CCPEs had stronger ability of disturbing the lipids than D-isomer.

3.8.2.   SAXS studies

The SAXS was used to further investigate the mechanism of permeation enhancing effects performed by MEN enantiomers (Fig. 10B). The diffraction peaks derived from the repeat distances of the lamellar structures of intercellular lipids. The two partially overlapped peaks originated from long and short lamellar structures and their repeat distances were calculated by Bragg's Law in Fig. 10E. The repeat distances of the long and short lamellar structures were approximately 13 nm (long-periodicity phase) and 6 nm (short-periodicity phase), respectively, roughly in line with the previous studies [25,26]. Obviously, the results showed that S-FP+L-MEN mixture performed stronger impacts on the long lamellar structure (14.19 nm), compared to the R-FP+L-MEN mixture (13.88 nm). In the case of D-isomer, R-FP

group performed greater impact on long lamellar structure (14.03 nm) (Fig. S3). The L-LIN showed the more interaction with SC than L-LIM because of inducing more changes in repeat distances. According to the results, it was found that CCPEs led to changes of the long-periodicity phase in SC. The structure of long-periodicity phase was susceptible to changes of lipids [27]. Intercellular lipids were primarily composed of amphiphilic ceramides, of which polar groups were arranged with face-to-face to form the aqueous layers [28]. Thus, increase in repeat distance of long lamellar structure showed that a proportion of CCPEs interacted with head of lipids to insert into the aqueous layers. In fact, L-isomer was much easier to interacted with lipids in the presence of S-enantiomer than D-isomer.

3.8.3.   DSC study of SC

DSC analysis was utilized to further investigate the mechanism of chiral permeation enhancing effects (Fig. 10C). The changes of Gibbs free energy of each component were illustrated in Fig. 10F which reflected the compatibility between SC and chiral drug with CCPEs. The lower Gibbs free energy indicated the better compatibility. And therefore, it indicated that L-isomer of CCPEs could increase the compatibility with SC in skin, as the same as the above characterization, L-MEN significantly improve the compatibility of S-enantiomer with skin than R-enantiomer.

3.8.4.   AFM study and MDS

The AFM study was utilized to visualize the selective permeation enhancing effects of CCPEs. The topographic images (20 mm × 20 mm) of the skin sites applied by the mixture of FP and MEN enantiomers were collected in Fig. 11A and the corresponding roughness (Average Deviation) was calculated to quantify the impact of CCPEs on SC by Agilent Technologies Picoview mode Software in Table 4 [29,30]. The control sample that treatment of solvent without drug and permeation enhancers showed a relatively smooth and soft surface with roughness value of 110.79 nm. MEN increased the transcellular gaps that disturbed the lipids to improve the FP permeation. However, the ability of enhancing effects of L- and D-MEN was different in accordance with the above the results. The combination of L-MEN and S-FP or D-MEN R-FP had more obvious advantages than that of L-MEN and R-FP or D-MEN and S-FP from the morphologies image of SC that deep area increased. Additionally, the results of roughness indicated different interaction had the great effect on the surface of skin. The roughness of skin surface was 132.86 and 141.61 nm with application of R-FP and S-FP. And the roughness of skin surface changed significantly after applying the MEN. And the combination of L-MEN and S-FP or D-MEN and R-FP increased roughness more for the skin surface. Therefore, it concluded that the stronger interaction between FP enantiomers and MEN enantiomers would result in lower MEN that entered into SC to disturb lipids and play a role in permeation enhancing effects, which was consistent with the above characterization.

The CED value was calculated by MDS to further quantify the interaction strength between MEN enantiomers and chiral lipids (Fig. 11B). The higher CED values suggested the stronger interaction strength (Table 4). It indicated that the stronger interaction occurred L-MEN and S-isomer of NS
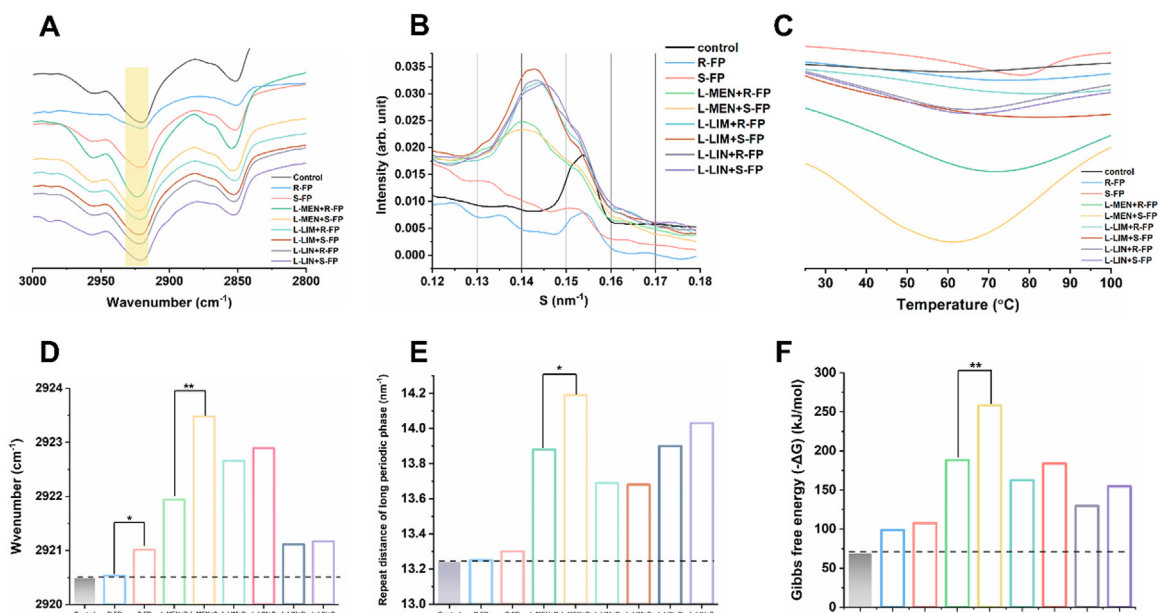
Fig. 10 – Characterization of skin with chiral drug and CCPEs. (A-B) ATR-FTIR profiles in the SC after treating with FP enantiomers and CCOEs, (B&E) SAXS profiles in the SC treated with FP enantiomers and CCPEs, (C&F) DSC curve of SC following by addition of FP enantiomers and CCPEs.

Table 4 – The roughness of skin surface and the CED values of MDS.

	Control	R-FP	S-FP	R-FP+L-MEN	S-FP+L-MEN	R-FP+D-MEN	S-FP+D-MEN
Roughness (nm)	110.79	132.86	141.62	210.32	268.90	200.29	251.45
CED×10^8 (J/m³)	/	1.31	1.39	1.42	1.51	1.47	1.40
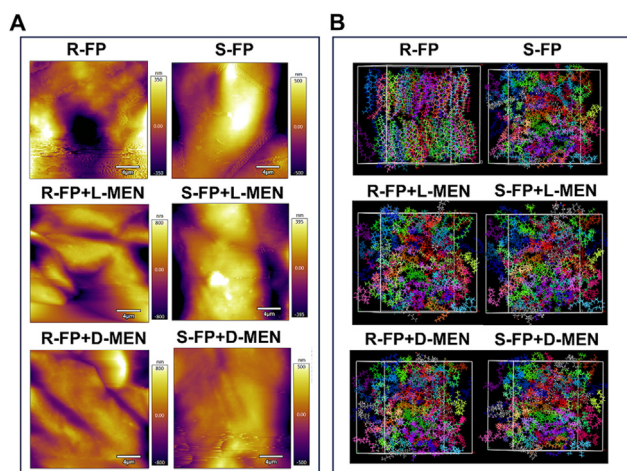
Fig. 11 – (A) AFM of Topography maps of skin samples under the treatment of FP and MEN enantiomers. (B) The snapshots of the simulated systems at the end stage of the MD.

in the presence of S-FP which disturbed the lipids in SC more apparently. On the other hand, the D-MEN had more disturbance effects on chiral NS in the presence of R-FP. In the SC lipids, L-MEN was easier to detach from the H-bond with the S-FP for better binding with the S-isomer of NS. As for D-MEN, it had opposite tendence with the R-FP.

In the present study, we investigated the law of enantioselective permeation enhancing effects of CCPEs on chiral drugs in TDDS and clarified their molecular mechanism by chiral drug-CCPEs and CCPEs-skin chiral interaction. In this study, we found that D-isomer of CCPEs enhanced the skin absorption of R-enantiomer of chiral NSAIDs (IB, FP, NP), of which D-MEN showed the best effects on it by higher partition and retention. On the other hand, L-isomer of CCPEs showed excellent enhancing effects on S-enantiomer of chiral NSAIDs (IB, FP, NP), in which L-MEN showed the best effects and the IVIVC by high retention and partition. The chiral conformation of CCPEs and drug enantiomers was dominant in this process ascribing to the polar group attached with the chiral center during the formation of H-bond.

We found that certain groups connected with the chiral carbon of drug enantiomers have impacts on H-bond strength with CCPEs stemming from the various steric hindrance that they produced, which was the key consideration in enantioselective permeation enhancing effects of CCPEs. This would change the release and partition of chiral drug and CCPEs from the preparation to skin (Fig. 2 and 4) that weaker chiral H-bond interaction between L-isomer of CCPEs and S-enantiomer of drug resulted in more release and partition. In general, CPEs have to experience two processes for work: (i)

Drugs and enhancers detached from the interaction between each other in matrix followed by entering into the skin. (ii) CPEs inserted into skin to disturb the lipids by CPEs-lipid molecular interaction and improve the transdermal drug permeation [23].

Firstly, the chiral drug-CCPEs interaction was capable of influencing the rate and extent of release of drugs from the matrix to the skin [31,32]. The presence of stronger chiral H-bond complex with higher degree of optical asymmetry between R-FP and L-MEN or S-FP and D-MEN suggested that different chiral conformation inhibited the electron transition surrounding the chiral centers (Fig. 9). The ^{13}C NMR experiments and MD shed light on the enantioselective mechanism that the different chiral interaction was attributed to the various chiral configurations of drug and CCPEs. In the case of L-MEN, on one hand, the methyl group of chiral carbon (C_2) in R-FP was away from the MEN molecules making it bring its carboxyl group as H-bond donor very close to hydroxyl of L-MEN to form the stronger H-bond (3.274 Å) (Fig. 8A). On the other hand, in the process of interacting S-FP with L-MEN, steric hindrance of methyl of C_2 in S-FP impeded the closer binding between them, as was evident by the C_3 chemical shift of S-FP (Fig. 7A). C_3 of S-FP was closer to the L-MEN, of which $C_{6'}$ showed partially positively charge resulting from the electron-withdrawing effects of oxygen atom, so that electron-cloud density around the methyl group of C_2 from S-FP was reduced and increased its chemical shift. Thus, the H-bond strength between L-MEN and S-FP was not as strong as that with R-FLU, attributing to the steric hindrance of methyl group connected with the chiral carbon atom of FP.

For D-MEN, since $C_{2'}$ of D-MEN was an R configuration, the isopropyl group connected to it acted as a block to hinder the binding of flurbiprofen enantiomers to D-MEN. Since the presence of larger hindrance provided by isopropyl groups linked to $C_{2'}$ of D-MEN made the steric hindrance effects of methyl groups linked to the chiral carbon of FP less effective, the strength of the interaction between D-MEN and FP enantiomers only depends on the distance of the groups forming hydrogen bonds according to the different steric position (Fig. S2). The weaker chiral interaction decreased the transdermal activation energy, in other words, it was easier for L-MEN to be pulled free of H-bond interaction with S-enantiomers than R-enantiomers and increase permeation amount of S-FP by inserting into tail of lipid molecular and interacting with head of lipids in SC [33] and the mechanism also pertained to both R-FLU and D-MEN as illustrated in Fig. 12.

In comparison with the L-MEN, L-LIM and LIN failed to perform the significantly enantioselective interaction with a pair of FP enantiomers. On one hand, L-LIM enantiomers without HBD and HBA was impossible to interact with the FP enantiomers by H-bond, suggesting that the certain groups attached with the chiral center struggle to play role in this process (Fig. 7B and 8B). Nevertheless, addition of L-LIM in transdermal formulation increased the concentration gradient that improve the partition and release of FP and CPEs toward skin. Numerous L-LIM accumulating in the skin disturbed the lipids pathway of SC that decreased the retention of drug and facilitated permeation of FP enantiomers. On the other hand, in terms of L-LIN
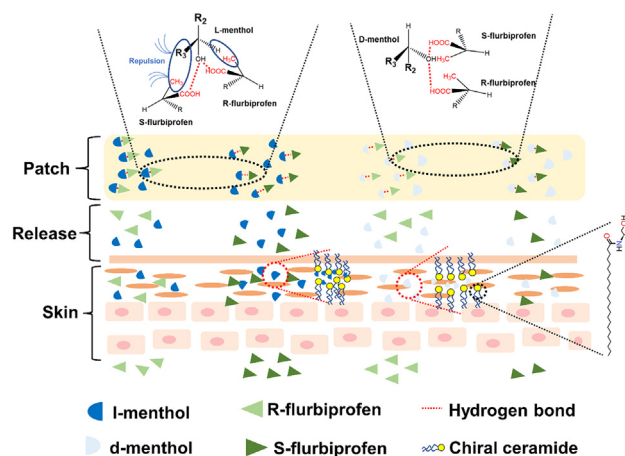
Fig. 12 – Schematic illustration of mechanistic insight of enantioselective permeation enhancing effects.

enantiomers with one chiral center, drug enantiomer could be able to form H-bond with them from any advantageous angle for the optimal conformation of H-bond complex, difficult to perform different chiral interaction between them. And thus, the H-bond decreased the release and partition of FP enantiomers and L-LIN, but the HBD that chiral LIN had was easier to insert into the lipids in SC to increase retention and permeation (Fig. 2, 7C and 8C).

In the second process that CCPEs-chiral skin interaction, CCPEs with different steric conformation disturbed chiral SC with varying degrees, which widened the difference of skin permeation between FP enantiomers. L-isomer was much easier to enter the hydrophilic region from the hydrophobic region and disturb the barrier function [34] and it was obtained that L-isomer of CCPEs had more permeation enhancing effects than D-isomer. The chiral ceramide abundant in SC was S-conformation [35]. And the interaction groups attached with the L-isomer of CCPEs was R-conformation, and thus, the enantiomeric relationship in space between them facilitated the bind (Fig. 10B), plus the weaker H-bond with S-enantiomer of S-FP, resulting better compatibility with SC (evident by the Gibbs free energy) (Fig. 10C) for better permeation and retention. On the other hand, S-conformation that D-isomer of CCPEs struggled to interact with S-ceramide which suggested that weaker interaction with lipids, based on the weaker H-bond with R-enantiomer, enabling it lower retention and better permeation (Fig. 11, S3 and S4). Lipids in SC primarily comprised of the ceramides, cholesterol and a small amount of fatty acid [36–38]. Pooja et al. reported that D-MEN was capable of strongly interacting with the cholesterol in biomembrane models to increase irritation [39]. Therefore, in addition to inserting into lipids, D-isomer can also interact with cholesterol to further weaken the barrier function of SC.

Therefore, as long as chiral drug and CCPEs was involved in the design of transdermal formulation, the interaction between them threatened to result in the enantioselective permeation of drug enantiomers. The clarification of enantioselective permeation enhancing effects in TDDS were extremely helpful when chiral excipients were introduced in transdermal formulation, which was necessary to consider

the influence of chiral excipients on chiral drugs. The appropriate choice of optically CPEs enantiomer for desired single drug enantiomer contributed to enhancing transdermal permeation, reducing intake of distomers and improving the therapeutic effects of the transdermal preparation.

4. Conclusion

In the present study, we investigated the law and molecular mechanism of enantioselective permeation enhancing effects of CCPEs on drug enantiomers in TDDS from perspective of chiral drug-CCPEs and CCPEs-chiral skin interaction. L-isomer of CCPEs could enhance the permeation of S-enantiomer by increased retention, in which L-MEN performed the outstanding effects by facilitating partition and retention of S-conformation. On the other hand, D-isomer of CCPEs enhance R-enantiomer by decreasing the skin retention where D-MEN showed the best effects that facilitate the partition of R-conformation. Non-chiral interaction between chiral drug-CCPEs failed to result in significant permeation enhancing effects. In the presence of chiral H-bond interaction, weaker H-bond interaction between S-enantiomer and L-MEN caused by the larger steric hindrance of chiral conformation increased the partition of FP and MEN toward skin. On the other hand, CCPEs-chiral skin interaction, different affinity between D- or L-MEN and chiral polar head groups of ceramides in SC, produced various permeation enhancing effects. This study was the first time to reveal the enantioselective enhancing permeation mechanism of CCPEs for chiral drugs in detail and provided a theoretical basis for the design of transdermal formulation containing chiral components.

Conflicts of interest

The authors declare that they have no known competing financial interests or personal relationships that could have appeared to influence the work reported in this paper.

Acknowledgements

Supplementary materials

Supplementary material associated with this article can be found, in the online version, at doi:10.1016/j.ajps.2023.100849.

References

[1] Kopečná M, Macháček M, Nováčková A, Paraskevopoulos G, Roh J, Vávrová K. Esters of terpene alcohols as highly potent, reversible, and low toxic skin penetration enhancers. Sci Rep 2019;9:14617.

[2] Boix-Montañés A, Celma-Lezcano C, Obach-Vidal R, Peraire-Guitart C. Collaborative permeation of drug and excipients in transdermal formulations. *In vitro* scrutiny for ethanol:limonene combinations. Eur J Pharm Biopharm 2022;181:239–48.

[3] Challener CA. Expanding the chiral toolbox. Pharm Technol 2016;40:28–9.

[4] Brooks WH, Guida WC, Daniel KG. The significance of chirality in drug design and development. Curr Top Med Chem 2011;11(7):760–70.

[5] Song L, Pan M, Zhao R, Deng J, Wu Y. Recent advances, challenges and perspectives in enantioselective release. J Control Release 2020;324:156–71.

[6] Olivella MS, Lhez L, Pappano NB, Debattista NB. Effects of dimethylformamide and L-menthol permeation enhancers on transdermal delivery of quercetin. Pharm Dev Technol 2007;12(5):481–4.

[7] Narishetty ST, Panchagnula R. Transdermal delivery of zidovudine: effect of terpenes and their mechanism of action. J Control Release 2004;95(3):367–79.

[8] Kommuru TR, Khan MA, Reddy IK. Effect of chiral enhancers on the permeability of optically active and racemic metoprolol across hairless mouse skin. Chirality 1999;11(7):536–40.

[9] Chen J, Jiang QD, Chai YP, Zhang H, Peng P, Yang XX. Natural terpenes as penetration enhancers for transdermal drug delivery. Molecules 2016;21(12):1709.

[10] Notman R, den Otter WK, Noro MG, Briels WJ, Anwar J. The permeability enhancing mechanism of DMSO in ceramide bilayers simulated by molecular dynamics. Biophys J 2007;93(6):2056–68.

[11] Thind R, O'Neill DW, Del Regno A, Notman R. Ethanol induces the formation of water-permeable defects in model bilayers of skin lipids. Chem Commun (Camb) 2015;51(25):5406–9.

[12] Kunta JR, Goskonda VR, Brotherton HO, Khan MA, Reddy IK. Effect of menthol and related terpenes on the percutaneous absorption of propranolol across excised hairless mouse skin. J Pharm Sci 1997;86(12):1369–73.

[13] Akhlaq M, Khan GM, Wahab A, Khan A, Hussain A, Nawaz A, et al. A simple high-performance liquid chromatographic practical approach for determination of flurbiprofen. J Adv Pharm Technol Res 2011;2(3):151–5.

[14] Geerts H. Drug evaluation: (R)-flurbiprofen–an enantiomer of flurbiprofen for the treatment of Alzheimer's disease. IDrugs 2007;10(2):121–33.

[15] Liu JK, Patel SK, Gillespie DL, Whang K, Couldwell WT. R-flurbiprofen, a novel nonsteroidal anti-inflammatory drug, decreases cell proliferation and induces apoptosis in pituitary adenoma cells *in vitro*. J Neurooncol 2012;106(3):561–9.

[16] Zhang Y, Liu C, Xu W, Quan P, Luo Z, Yang D, et al. An investigation on percutaneous permeation of flurbiprofen enantiomers: the role of molecular interaction between drug and skin components. Int J Pharm 2021;601:120503.

[17] Tian Q, Quan P, Fang L, Xu H, Liu C. A molecular mechanism investigation of the transdermal/topical absorption classification system on the basis of drug skin permeation and skin retention. Int J Pharm 2021;608:121082.

[18] Goh CF, Hadgraft J, Lane ME. Thermal analysis of mammalian stratum corneum using differential scanning calorimetry for advancing skin research and drug delivery. Int J Pharm 2022;614:121447.

[19] Danzberger J, Donovan M, Rankl C, Zhu R, Vicic S, Baltenneck C, et al. Glycan distribution and density in native skin's stratum corneum. Skin Res Technol 2018;24(3):450–8.

[20] Krishnaiah YS, Kumar MS, Raju V, Lakshmi M, Rama B. Penetration-enhancing effect of ethanolic solution of menthol on transdermal permeation of ondansetron hydrochloride across rat epidermis. Drug Deliv 2008;15(4):227–34.

[21] Cornwell PA, Barry BW. The routes of penetration of ions and 5-fluorouracil across human skin and the mechanisms of action of terpene skin penetration enhancers. Int J Pharm 1993;94(1–3):189–94.

[22] Kamatou GP, Vermaak I, Viljoen AM, Lawrence BM. Menthol: a simple monoterpene with remarkable biological properties. Phytochemistry 2013;96:15–25.

[23] Luo Z, Liu C, Quan P, Zhang Y, Fang L. Effect of chemical penetration enhancer-adhesive interaction on drug release from transdermal patch: mechanism study based on FT-IR spectroscopy, ^{13}C NMR spectroscopy, and molecular simulation. AAPS PharmSciTech 2021;22(5):198.

[24] Yang D, Liu C, Quan P, Fang L. A systematic approach to determination of permeation enhancer action efficacy and sites: molecular mechanism investigated by quantitative structure-activity relationship. J Control Release 2020;322:1–12.

[25] Hill JR, Wertz PW. Molecular models of the intercellular lipid lamellae from epidermal stratum corneum. Biochim Biophys Acta 2003;1616(2):121–6.

[26] McIntosh TJ. Organization of skin stratum corneum extracellular lamellae: diffraction evidence for asymmetric distribution of cholesterol. Biophys J 2003;85(3):1675–81.

[27] Feingold K, Elias P. The important role of lipids in the epidermis and their role in the formation and maintenance of the cutaneous barrier. Biochim Biophys Acta 2014;1841(3):279.

[28] Levine YK, Wilkins MH. Structure of oriented lipid bilayers. Nat New Biol 1971;230(11):69–72.

[29] Chen S, Bhushan B. Nanomechanical and nanotribological characterization of two synthetic skins with and without skin cream treatment using atomic force microscopy. J Colloid Interface Sci 2013;398:247–54.

[30] Gorzelanny C, Goerge T, Schnaeker EM, Thomas K, Luger TA, Schneider SW. Atomic force microscopy as an innovative tool for nanoanalysis of native stratum corneum. Exp Dermatol 2006;15(5):387–91.

[31] Benson HA, Sarveiya V, Risk S, Roberts MS. Influence of anatomical site and topical formulation on skin penetration of sunscreens. Ther Clin Risk Manag 2005;1(3):209–18.

[32] Higuchi T. Physical chemical analysis of percutaneous absorption process from creams and ointments. J Soc Cosmet Chem 1960;11:85–97.

[33] Jain R, Aqil M, Ahad A, Ali A, Khar RK. Basil oil is a promising skin penetration enhancer for transdermal delivery of labetolol hydrochloride. Drug Dev Ind Pharm 2008;34(4):384–9.

[34] Chantasart D, Pongjanyakul T, Higuchi WI, Li SK. Effects of oxygen-containing terpenes as skin permeation enhancers on the lipoidal pathways of human epidermal membrane. J Pharm Sci 2009;98(10):3617–32.

[35] Kawana M, Miyamoto M, Ohno Y, Kihara A. Comparative profiling and comprehensive quantification of stratum corneum ceramides in humans and mice by LC/MS/MS. J Lipid Res 2020;61(6):884–95.

[36] Gray GM, White RJ, Williams RH, HJ Yardley. Lipid composition of the superficial stratum corneum cells of pig epidermis. Br J Dermatol 1982;106(1):59–63.

[37] Zhang Y, Chen J, Gong H, Zhou Y, Zhang J, Li M, Cui Y. Enantioselective evaluation of chiral cosmetic preservative chlorphenesin on cytotoxicity, pharmacokinetics and tissue distribution. Microchem J 2023;187:108460.

[38] Wang H, Li Y, Wang C, Wang J, Ren B, Li X, Li M, Geng D, Wu C, Zhao L. The enhancing effect and promoting mechanisms of the stereoisomeric monoterpene alcohol esters as enhancers for drugs with different physicochemical properties. Asian J Pharm Sci 2022;17(1):139–52.

[39] Gusain P, Ohki S, Hoshino K, Tsujino Y, Shimokawa N, Takagi M. Chirality-dependent interaction of d- and l-menthol with biomembrane models. Membranes (Basel) 2017;7(4):69.